

Performance & Analysis of Grid Connected Renewable Energy System with Multilevel NPC Inverter

Pankaj Sarsia¹ PhD. Scholar, EE, Prarthana Nagle²

AISECT University, M.tech S.A.T.I
Bhopal India Vidisha India

Abstract: In recent years, multilevel inverters have gained popularity with medium and high power ratings. Renewable energy sources such as photovoltaic, wind, and fuel cells can be interfaced to a multilevel converter system. Wind is one of the most abundant renewable sources of energy in nature. Wind energy can be harnessed by a wind energy conversion system (WECS) composed of a wind turbine, an electric generator, a power electronic converter and the corresponding control system. The most advanced generator type is perhaps the permanent magnet synchronous generator (PMSG). The wind energy is connected to ac grid connected load. When the grid is concerned the loads may be unbalanced and non-linear in nature. Hence, grid should not inject harmonic and unbalanced currents into the grid. Harmonic currents and negative sequence currents (due to unbalance) will unnecessary increase the line currents. These problems are solved by using effective controllers with multilevel inverters. Multilevel inverter is used to step up the voltage and to reduce the THD. Here nine level and eleven level inverter are used and the voltage increases and THD reduces from 12.87 % to 4.38 %. Active and reactive power is controlled dc stabilization and the reactive power is near to unity. Here LC filter is used to remove the harmonics available in the system. In order to evaluate the performance of the proposed approach, a model of the AC grid, non-linear load, multilevel inverter and renewable energy resources (e.g., wind power generation) had developed in MATLAB / SIMULINK environment.

Keywords: Wind Energy, PMSG, Total Harmonics Distortion, Multilevel Inverter.

I. INTRODUCTION

The increase of the world energy demand has entailed the investment of huge amounts of resources, economical and human, to develop new technologies capable to produce, transmit and convert all needed electric power. In addition, the dependence on fossil fuels and the progressive increase of its cost lead to appearance of new cheaper and cleaner energy resources not related to fossil fuels. In ultimate decades, renewable energy resources have been the focus for researchers, and different families of power converters have been designed to integrate these types of supplies into the distribution grid. Beside the generation, electric power transmission needs high power electronic systems to assure conversion and the energy quality. Numerous industry applications, such as for example textile and paper industry, steel mills, electric and hybrid electric vehicles, ship propulsion, railway traction, „more-electric“ aircraft, etc., require utilization of variable speed electric drives. As far as the variable speed operation of electric drives is concerned, this is nowadays invariably achieved by supplying the machine, regardless of the type, from a power electronic converter.

Therefore, power electronic converters have the responsibility to carry out these tasks with high efficiency. At each of these stages rapid development of the power electronic lead to implementation of new power converter topologies and semiconductor technologies. A continuous race to develop higher-voltage and higher-current power semiconductors to drive high-power

Systems still goes on. In this way, the last-generation devices are suitable to support high voltages and currents (around 6.5 kV and 2.5 kA). However, currently there is tough competition between the use of classic power converter topologies using high-voltage semiconductors and new converter topologies using medium-voltage devices. The multilevel converters built using mature medium-power semiconductors are competing with classic power converters using high-power semiconductors that are under continuous development and not mature. Indeed, multilevel converters using more switching components can be both cheaper and more reliable than standard two-level solution with rare and more expensive components. In addition, multilevel solution requires smaller filter to satisfy power quality requirements, which can be significant item in high-power range. Nowadays, multilevel converters are a good solution for power applications because they can achieve high power using mature medium-power semiconductor technology covering power range from 1 MW to 30 MW.

The maximum power limit of standard three-phase converters is related to the limits of the maximum voltage and current of a switching component. Furthermore, higher is the power of a switch lower is the switching frequency. An initial solution to overcome these limitations was connection of several switches in series or in parallel. The series connection of two or more semiconductor devices faces problems due to the difficulty

to synchronize perfectly their commutations. In fact, if one component switches off faster than the others it will blow up because it will be subject to the entire voltage drop designed for the series. Instead, parallel connection is slightly less complicated because of the positive resistance coefficient property of MOSFETs and IGBTs with the increment of junction temperature. When a component switches on faster than the others do, it will conduct a current greater than the rated one. In this way, the component increases its junction temperature and its resistance, in this way limiting the current to some extent. This effect makes possible to overcome the problems coming from a delay among gate signals or from differences among real turn on time of the components. Nevertheless, parallel connection of the switches has its limits: it requires careful I precise design of the system to achieve almost perfect symmetry of the components, a task more difficult to maintain as their number rises. Moreover, multilevel converters present several other advantages:

- Generate better output waveforms with a lower dv/dt than the standard converters (power quality).
- Increase the power quality due to the great number of levels of the output voltage: in this way, the AC side filter can be reduced, decreasing its costs and losses (low switching losses).
- Can operate with a lower switching frequency than two-level converters, so the electromagnetic emissions they generate are weaker, making less severe to comply with the standards (EMC).
- Can be directly connected to high voltage sources without using transformers; this means a reduction of implementation and costs.

The main disadvantages of this technique are:

- Larger number of semiconductor switches required increasing complexity compared to the two-level solution.
- Capacitor banks or insulated sources are required to create the dc voltage steps.

Multilevel converters are a viable solution to increase the power with a relatively low stress on the components and with simple control systems.

The most common multilevel converter topologies are [4]:

- Diode clamped (neutral-point clamped),
- Flying capacitor (capacitor-clamped),
- Cascaded topology.

II. MODELLING OF WIND TURBINE

The static characteristic of the turbine (output as a function of wind speed) can be described by the relationship between the total power and mechanical energy of the wind:

$$P_{wind} = \frac{1}{2} \rho \pi R_{turbine}^2 v_{wind}^3 \tag{1}$$

where ρ is the air density (1,225 kg/m³), $R_{turbine}$ is thenrotor radius (m), v_{wind} is the wind speed (m/s). It is impossible to extract all the kinetic energy of wind, so it extracts a fraction of the power of wind as shown in (2) as the power coefficient C_p .

$$P_m = \frac{1}{2} C_p \rho \pi R_{turbine}^2 v_{wind}^3 \tag{2}$$

P_m is the mechanical power of the wind (Nm/s). The maximum power coefficient C_{pM} is 0.59. This coefficient is also known as Betz limit. It can be expressed in terms of reduced velocity λ and angle of light θ : $C_p = C_p(\lambda, \theta)$.

If W is the rotor speed, the reduced speed λ is defined:

$$\lambda = \frac{\Omega R_{turbine}}{v_{wind}} \tag{3}$$

Assuming a constant wind speed v_{wind} , the reduced speed λ varies proportionally to the rotor speed [10]. The maximum value of C_p is generally obtained for values of λ around 8 to 9 (when the tip of the movements of blade is 8 to 9 times faster than the wind). On modern wind turbines, it is possible to adjust the angle of the blades through a control mechanism [11]. If C_p - λ curve is known for a specific wind with a radius of turbine rotor $R_{turbine}$, it is easy to construct the curve of C_p as a function of rotational speed Ω for a wind speed v_{wind} . The output torque of the turbine is calculated :

$$T_m = \frac{P_m}{\Omega} = \frac{1}{2} \frac{C_p \rho \pi R_{turbine}^2 v_{wind}^3}{\Omega} \tag{4}$$

If the speed ratio λ is maintained at its optimal value λ_{opt} , the power coefficient is at its maximum value $C_{pM}=C_p(\lambda_{opt})$, the maximum power of the wind turbine will be:

$$P_m^{opt} = \frac{1}{2} C_{pM} \rho \pi R_{turbine}^2 v_{wind}^3 \tag{5}$$

On the other hand, the speed ratio assumed to be maintained at the optimum value, we obtain the optimum speed rotor:

$$\lambda^{opt} = \frac{\Omega R_{turbine}}{v_{wind}} \Rightarrow \Omega^{opt} = \frac{\lambda^{opt} v_{wind}}{R_{turbine}} \tag{6}$$

Thus, the wind power turbine characteristics is shown in figure 2.1.

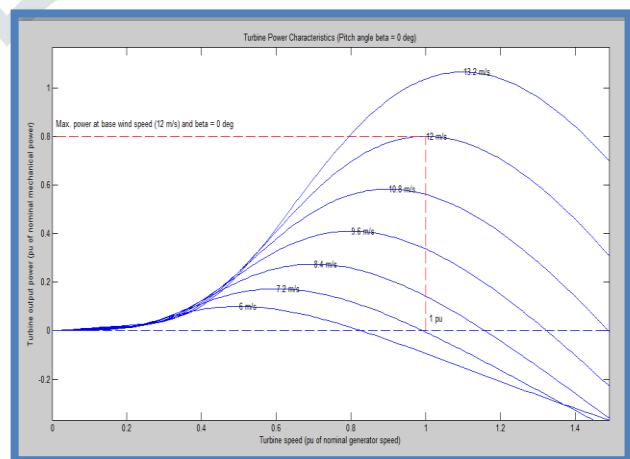


Figure 2.1: Wind Turbine Power Characteristics

In this paper, a wind turbine is simulated by using a look-up table, where inputs are wind speed and rotor speed and output is the mechanical torque.

III. MODELLING OF PMSM

The mathematical model for the vector control of the PMSM can be derived from its dynamic d-q model which can be obtained from well-known model of the induction machine with the equation of damper winding and field current dynamics removed. The synchronously rotating rotor reference frame is chosen so the stator winding quantities are transformed to the synchronously rotating reference frame that is revolving at rotor speed.

The model of PMSM without damper winding has been developed on rotor reference frame using the following assumptions:

- 1) Saturation is neglected.
- 2) The induced EMF is sinusoidal.
- 3) Core losses are negligible.
- 4) There are no field current dynamics.

It is also be assumed that rotor flux is constant at a given operating point and concentrated along the d axis while there is zero flux along the q axis, an assumption similarly made in the derivation of indirect vector controlled induction motor drives. The rotor reference frame is chosen because the position of the rotor magnets determine independently of the stator voltages and currents, the instantaneous induced emf and subsequently the stator currents and torque of the machine. When rotor references frame are considered, it means the equivalent q and d axis stator windings are transformed to the reference frames that are revolving at rotor speed. The consequences is that there is zero speed differential between the rotor and stator magnetic fields and the stator q and d axis windings have a fixed phase relationship with the rotor magnet axis which is the d axis in the modelling. The stator equations of the induction machine in the rotor reference frames using flux linkages are taken to derive the model of the PMSM as shown in Fig.3.1:

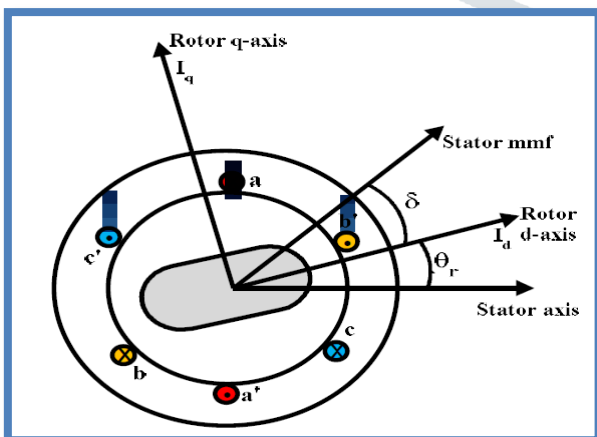


Fig.3.1: PM machine synchronously rotating d-q reference frame.

So an PM machine is described by the following set of general equations:

Voltage equations are given by:

$$\begin{aligned} V_d &= R_s i_d - \omega_r \lambda_q + \frac{d\lambda_d}{dt} \\ V_q &= R_s i_q - \omega_r \lambda_d + \frac{d\lambda_q}{dt} \end{aligned} \tag{1}$$

Flux linkages are given by

$$\begin{aligned} \lambda_q &= L_q i_q \\ \lambda_d &= L_d i_d + \lambda_f \end{aligned} \tag{3}$$

Substituting (3) & (4) into (1) & (2), we get

$$V_q = R_s i_q + \omega_r (L_d i_d + \lambda_f) + \frac{d}{dt} (L_q i_q) \tag{5}$$

$$V_d = R_s i_d - \omega_r L_q i_q + \frac{d}{dt} (L_d i_d + \lambda_f) \tag{6}$$

Arranging equations (5) and (6) in matrix form

$$\begin{pmatrix} V_q \\ V_d \end{pmatrix} = \begin{pmatrix} R_s + \frac{dL_q}{dt} & \omega_r L_d \\ -\omega_r L_q & R_s + \frac{dL_d}{dt} \end{pmatrix} \begin{pmatrix} i_q \\ i_d \end{pmatrix} + \begin{pmatrix} \omega_r \lambda_f \\ \frac{d\lambda_f}{dt} \end{pmatrix}$$

The developed torque motor is being given by

$$T_e = 3/2 (P/2) (\lambda_d i_q - \lambda_q i_d) \tag{8}$$

$$T_e = 3/4 P [\lambda_f i_q + (L_d - L_q) i_q i_d] \tag{9}$$

The mechanical torque equation is

$$T_e = T_L + B\omega_m + J \frac{d\omega_m}{dt} \tag{10}$$

Solving for rotor mechanical speed from (10), we get

$$\omega_m = \frac{1}{J} (T_e - T_L - B\omega_m) dt \tag{11}$$

and rotor electrical speed is $\omega_r = \omega_m (P/2)$. (12)

IV. MULTILEVEL INVERTER TOPOLOGY

Neutral Point-Clamped Inverter:

A three-level diode-clamped inverter is shown in Fig. 4.1(a). In this circuit, the dc-bus voltage is split into three levels by two series-connected bulk capacitors, C1 and C2. The middle point of the two capacitors n can be defined as the neutral point. The output voltage van has three states: Vdc/2, 0, and -Vdc/2. For voltage level Vdc/2, switches S1 and S2 need to be turned on; for -Vdc/2, switches S1" and S2" need to be turned on; and for the 0 level, S2 and S1" need to be turned on.

The key components that distinguish this circuit from a conventional two-level inverter are D1 and D1". These two diodes clamp the switch voltage to half the level of the dc-bus voltage. When both S1 and S2 turn on, the voltage across a and 0 is Vdc i.e., $v_{a0} = Vdc$. In this case, D1" balances out the voltage sharing between S1" and S2" with S1" blocking the voltage across C1 and S2" blocking the voltage across C2. Notice that output voltage van is ac, and v_{a0} is dc. The difference between van and v_{a0} is the voltage across C2, which is $Vdc/2$. If the output is removed out between a and 0, then the circuit becomes a dc/dc converter, which has three output voltage levels: Vdc, Vdc/2, and 0.

Considering that m is the number of steps of the phase voltage with respect to the negative terminal of the inverter, then the number of steps in the voltage between two phases of the load k is

$k = 2m+1$ (1) and the number of steps p in the phase voltage of a three-phase load in wye connection is $p = 2k - 1$. (2)

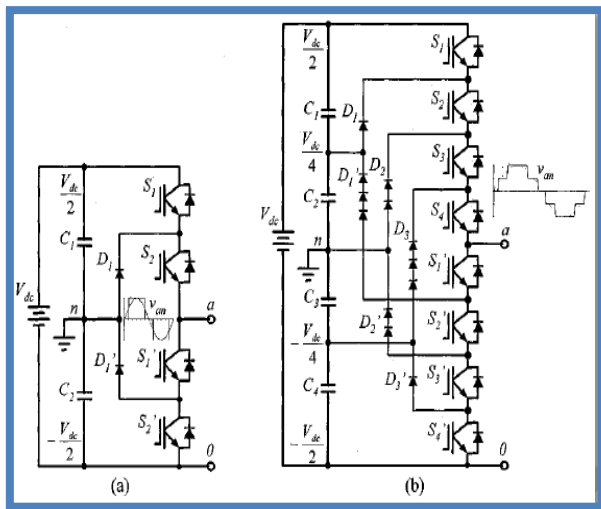


Fig. 4.1. Diode-clamped multilevel inverter circuit topologies.(a) Three-level. (b) Five-level.

The term multilevel starts with the three-level inverter introduced by Nabae et al. [3]. By increasing the number of levels in the inverter, the output voltages have more steps generating a staircase waveform, which has a reduced harmonic distortion. However, a high number of levels increases the control complexity and introduces voltage imbalance problems.

Fig. 4.1(b) shows a five-level diode-clamped converter in which the dc bus consists of four capacitors, C1, C2, C3, and C4. For dc-bus voltage V_{dc} , the voltage across each capacitor is $V_{dc}/4$, and each device voltage stress will be limited to one capacitor voltage level $V_{dc}/4$ through clamping diodes. To explain how the staircase voltage is synthesized, the neutral point n is considered as the output phase voltage reference point. There are five switch combinations synthesize five level voltages across a and n .

- 1) For voltage level $V_{an} = V_{dc}/2$, turn on all upper switches S_1-S_4 .
- 2) For voltage level $V_{an} = V_{dc}/4$, turn on three upper switches S_2-S_4 and one lower switch S_1' .
- 3) For voltage level $V_{an} = 0$, turn on two upper switches S_3 and S_4 and two lower switches S_1' and S_2' .
- 4) For voltage level $V_{an} = -V_{dc}/4$, turn on one upper switch and three lower switches $S_1'-S_3'$.
- 5) For voltage level $V_{an} = -V_{dc}/2$, turn on all lower switches $S_1'-S_4'$.

Four complementary switch pairs exist in each phase. The complementary switch pair is defined such that turning on one of the switches will exclude the other from being turned on. In this example, the four complementary pairs are (S_1, S_1') , (S_2, S_2') , (S_3, S_3') , and (S_4, S_4') .

Although each active switching device is only required to block a voltage level of $V_{dc}/(m-1)$, the clamping diodes must have different voltage ratings for reverse voltage blocking. Using D_1' of Fig. 2(b) as an example, when lower devices $S_2' \sim S_4'$ are turned on, D_1' needs to block

TABLE I. SWITCHING STATES OF THE FIVE LEVEL INVERTER

Output V_{a0}	Switch States							
	S_1	S_2	S_3	S_4	S_1'	S_2'	S_3'	S_4'
$V_3 = V_{dc}$	1	1	1	1	0	0	0	0
$V_4 = 3V_{dc}/4$	0	1	1	1	1	0	0	0
$V_5 = V_{dc}/2$	0	0	1	1	1	1	0	0
$V_6 = V_{dc}/4$	0	0	0	1	1	1	1	0
$V_7 = 0$	0	0	0	0	1	1	1	1

three capacitor voltages, or $3V_{dc}/4$. Similarly, D_2' and D_2'' need to block $2V_{dc}/4$, and D_3 needs to block $3V_{dc}/4$. Assuming that each blocking diode voltage rating is the same as the active device voltage rating, the number of diodes required for each phase will be $(m-1)(m-2)$. This number represents a quadratic increase in m . When m is sufficiently high, the number of diodes required will make the system impractical to implement. If the inverter runs under PWM, the diode reverse recovery of these clamping diodes becomes the major design challenge in high-voltage high-power applications.

V. SIMULATION & RESULTS

The simulation system of 11 level NPC multi-level inverter with renewable energy resources in to AC grid is validated by simulation of the circuit in MATLAB/SIMULINK environment.

The entire wind energy conversion system is as shown in figure. The blades of the turbine capture wind energy and transfer energy to the turbine rotor which is connected to a common shaft connecting the PMSG. PMSG converts this mechanical energy to three phase ac voltage which fluctuates according to the wind speed. This three phase ac voltage is converted into dc by a three phase rectifier. Output dc voltage is fed to a boost converter which boosts the input signal voltage and feeds an amplified dc voltage to the MLI. The NPC topology of the MLI blocks the dc component from entering the grid and provides feasible application of control technique for the switches.

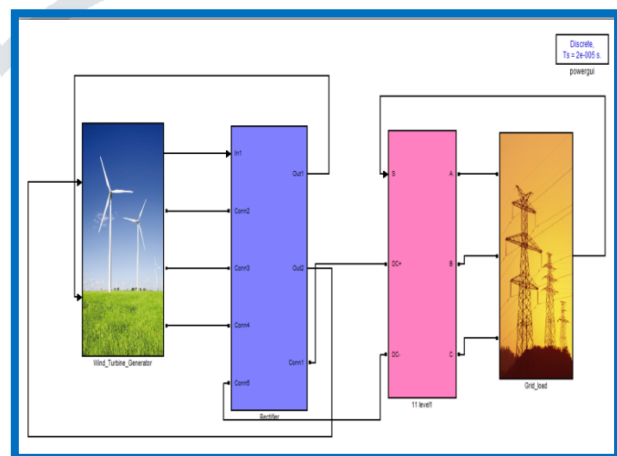


Figure 5.1: Schematic Model of AC grid connected renewable energy resources with NPC Multi Inverter

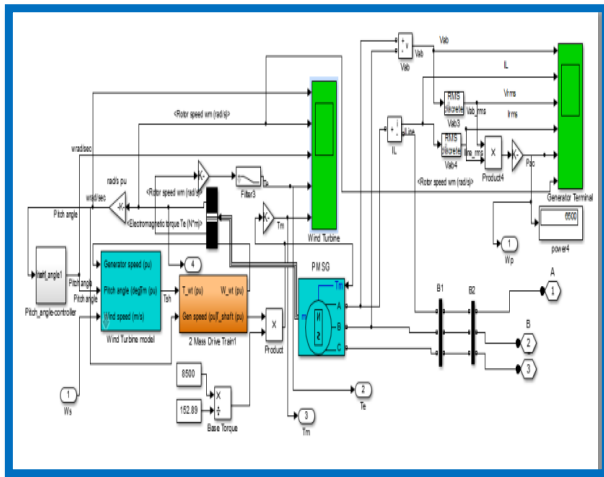


Figure 5.2: Wind power generation by using PMSG

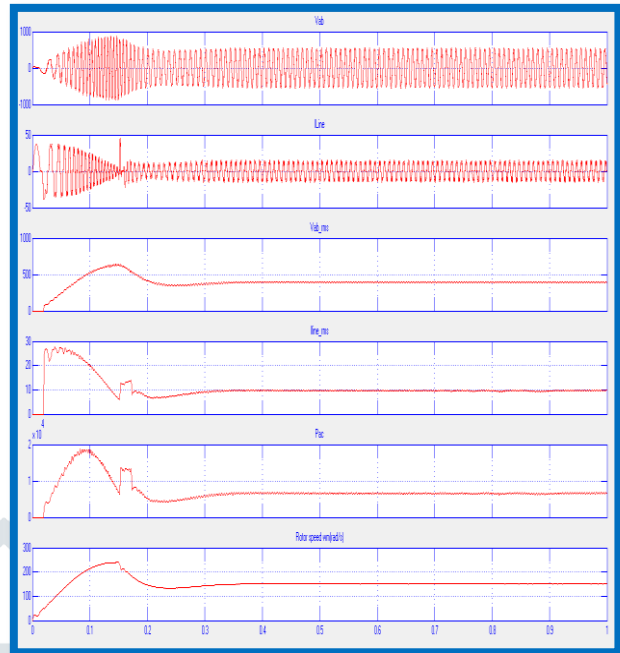


Figure 5.5: Waveform of Generator Terminal (a) Voltage at stator terminal of ab (b) Current of Line (c) RMS Voltage at stator terminal of ab (d) RMS current of Line (e) Generated Power (f) Rotor Speed.

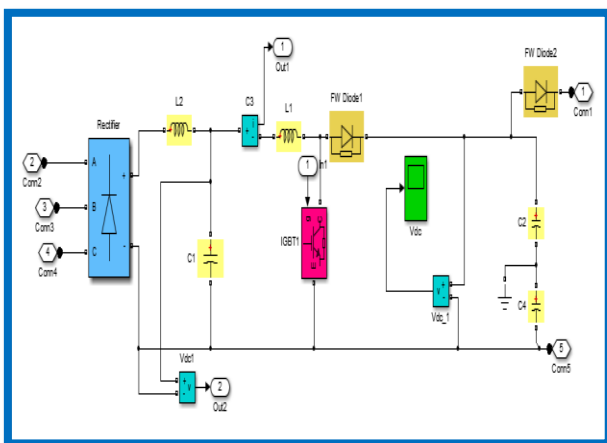


Figure 5.3: Simulink of Rectifier

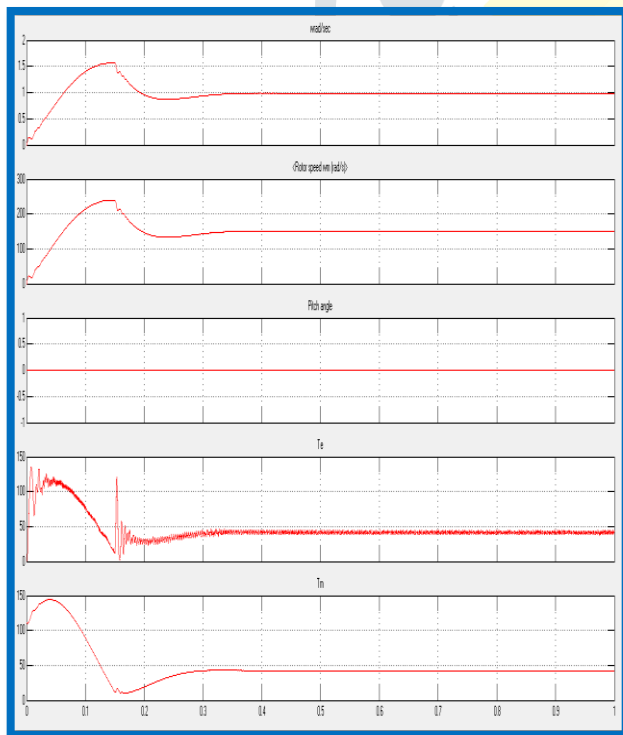


Figure 5.4: Waveform of Wind Turbine (a) wind Speed (b) Rotor speed (c) Pitch angle (d) Electromagnetic Torque (e) Mechanical Torque.

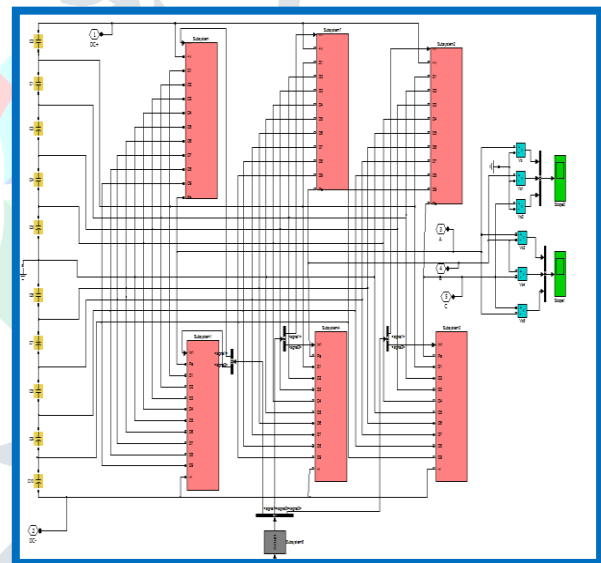


Figure 5.6: Simulink model of 11 level NPC multi inverter

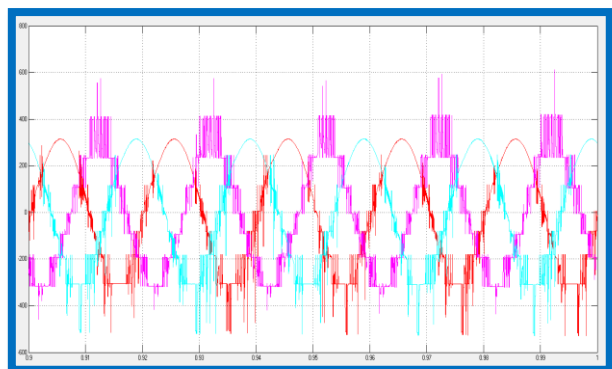


Figure 5.7: Output waveform of Upper half 11 level NPC multi inverter

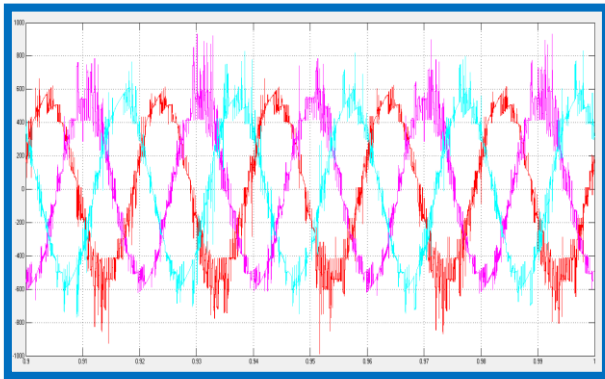


Figure 5.8: Output waveform of Lower half 11 level NPC multi inverter

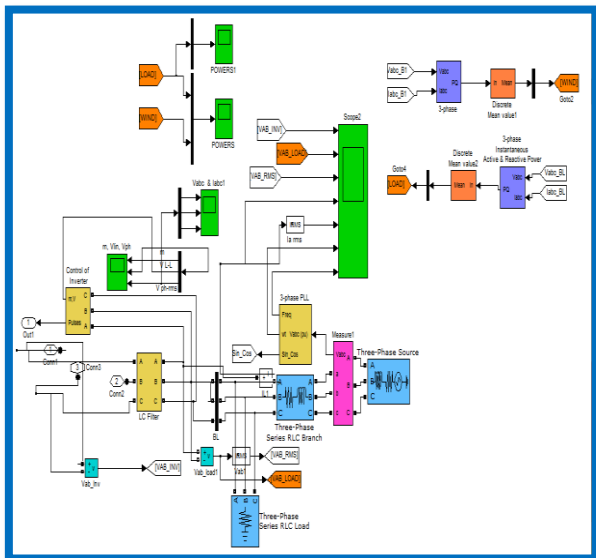


Figure 5.9: Simulink Model of AC Grid Connected Load

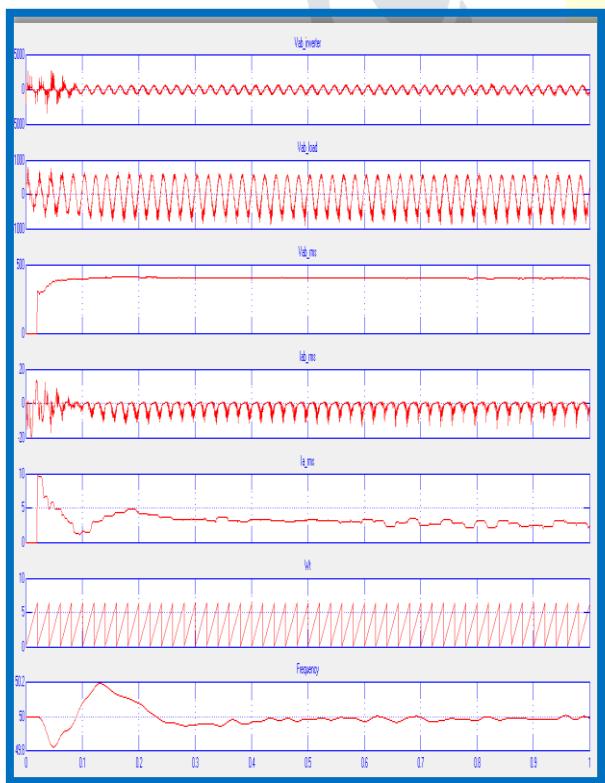


Figure 5.10: Waveform of AC Grid Connected Load (a) Voltage at Inverter (b) Voltage at Load (c) RMS Voltage at Inverter (d) RMS current of Load at terminal ab (e) RMS current of Load at terminal ab (f) Rotor Speed (g) Frequency .

VI. CONCLUSION

In this paper, the performance of eleven levels NPC inverter to integrate renewable energy resource in to AC grid was presented. Using Eleven level NPC Converter, the whole system will declines output harmonic effectively while improving power capacity of whole equipment, and reducing the voltage stress of switch and the equivalent switching frequency. As the wind speed varies the voltage and current also varies these affects , the grid power as speed are going to decreased, the active and reactive power also decreasing the pitch angle controller is used to control the blade angle at $\theta = 0$. Simulations show that generator side can realize the maximum wind power tracking, and makes the generator operate stably and efficiently by using double closed loop control based on maximum ratio of torque to current. The grid side converter adopts the vector control of grid voltage orientation, realizing the decoupling control of the active and reactive power. While feed in grid high quality electrical energy, it also improves the utilization of the whole system. Here the LC filter is used to remove the harmonics available in the system. The MPPT is used to track the maximum power. From the above we can conclude that as the level of inverter increases line and phase voltage waveform is increases and the harmonic induced is decreases. Simulation results clarified the ability of control scheme in compensation of load active and reactive power. We can observe that for eleven level NPC inverter THD is less compared to nine level NPC inverter as interfacing circuit to integrate renewable energy in to AC grid. From the FFT analysis of nine level NPC inverter and eleven level NPC inverter the THD of nine level is 12.87% which has more than eleven level NPC inverter is 4.38% i.e. as the level of inverter increases THD decreases. The proposed control scheme has the ability to be used in all types of converter topologies and can be used as a multi objective strategy for integration of renewable energy resources in to AC grids.

REFERENCES

- [1]. A. Nasiri, O. Abdel-Baqi, and B. Novakovic, "A Hybrid System of Li-Ion Capacitors and Flow Battery for Dynamic Wind Energy Support," IEEE 2013.
- [2]. A. Nabae, I. Takahashi, and H. Akagi, "A new neutral-point clamped PWM inverter," IEEE Trans. Sep. 1981.
- [3]. AkieUehara, AlokPratap, Tomonori Goya. A Coordinated Control Method to Smooth Wind Power Fluctuations of a PMSG-Based WECS[J].IEEE Transactions on Energy Conversion, Vol.26,No.2, 2011
- [4]. B. Boukhezzer and H. Siguerdidjane, "Nonlinear control of a variable-speed wind turbine using a two-mass model," IEEE Trans. 2011.
- [5]. B. M. Delghavi, A. Yazdani, "An Adaptive Feedforward Compensation for Stability Enhancement in Droop-Controlled Inverter-Based Microgrids," IEEE Transactions on Power Delivery 2011.
- [6]. Edris Poursmaeil, Daniel Montesinos-Miracle, and Oriol Gomis Bellmunt "Control Schem of Three-Level NPC Inverter for

- Integration of Renewable Energy Resources into AC Grid""', IEEE 2012.
- [7]. F. Carnielutti, H. Pinheiro, and C. Rech, "Generalized carrier-based modulation strategy for cascaded multilevel converters operating under fault conditions," IEEE Trans. Ind. Electron Feb. 2012.
- [8]. G. Delille, B. Francois, and G. Malarange, "Dynamic Frequency Control Support by Energy Storage to Reduce the Impact of Wind and Solar Generation on Isolated Power System's Inertia," IEEE 2012.
- [9]. G. Mandic and A. Nasiri "Modeling and Simulation of a Wind Turbine System with Ultracapacitors for Short-Term Power Smoothing," in Proc. IEEE International Symposium on Industrial Electronics, July 2010 Italy.
- [10]. L. Serpa, S. Ponnaluri, P. Barbosa, J. Kolar, "A modified direct power control strategy allowing the connection of three-phase inverters to the grid through LCL filter," IEEE 2007, Page(s) 1388-1400.
- [11]. Mukhtiar Singh, Vinod Khadkikar, Ambrish Chandra, and Rajiv K. Varma, "Grid Interconnection of Renewable Sources at the Distribution Level With Power Quality Improvement Features", IEEE 2011.
- [12]. N. R. Ullah, T. Thiringer, and D. Karlsson, "Voltage and Transient Stability Support by Wind Farms Complying With the E.ON Netz Grid Code," IEEE Transactions on Power Systems, vol. 22, no. 4, pp. 1647-1656, 2007.
- [13]. S. Alepuz, S. Busquets-Monge, J. Bordonau, J. Gago, D. Gonzalez, and J. Balcells, "Interfacing renewable energy source to the utility grid using a three-level inverter," IEEE Trans. Ind Oct. 2006.
- [14]. Xu Lie; Zhi Dawei; Yao Liangzhong; "Direct power control of grid connected voltage source converters," IEEE Power engineering society general meeting, pp. 1-6, 2007

